brief communication

Recognition processes at a functionalized lipid surface observed with molecular resolution

David Vaknin,* Jens Als-Nielsen,* Michael Piepenstock,‡ and Mathias Lösche‡
*Physics Department, Risø National Laboratory, DK-4000 Roskilde, Denmark and ‡Institute of Physical Chemistry, Johannes-Gutenberg-Universität Mainz, D-6500 Mainz, Germany

ABSTRACT The specific binding of proteins to functionalized lipid monolayers on aqueous subphases was characterized by neutron reflectivity and fluorescence microscopy measurements. Due to the high affinity and high specificity of their noncovalent interaction, streptavidin (SA) and biotin (vitamin H) were chosen as a model system to investigate the structural characteristics of a recognition process on a molecular length scale. Changes in the neutron reflection from the surfaces of NaCl aqueous (H_2O or D_2O) protein solutions (10^{-8} M SA) were used to monitor the interaction of the protein with a monolayer of a biotinylated lipid in situ. Refinement of the reflectivity data and independent fluorescence microscopic observation of the interface using FITC-labeled SA showed that the protein forms macroscopically homogeneous (and presumably crystalline) domains covering a large portion of the surface. Moreover, the neutron reflection experiments clearly showed the formation of a monomolecular protein layer with an effective thickness, $d_p = 43.7 \pm 2$ Å. The area per protein molecule occupied in the film was $A_0 = 2860 \pm 200$ Å^2 and $n_w = 260 \pm 100$ water molecules were associated with each protein molecule. Quantitative binding was found to occur at biotin surface concentrations as low as 1 molecule/1,250 Å^2 (compared with ~1 molecule/40 Å^2 for dense packing). This study demonstrates the application of a promising new tool for the systematic investigation of molecular recognition processes in protein/lipid model systems.

INTRODUCTION

Streptavidin, a tetrameric protein isolated from *Streptomyces avidinii* (1), has been employed universally in biotechnology. That is due to its exceptionally high affinity ($K_a \sim 10^{15}$ M^{-1}) (2) to biotin, which is similar in its stability to covalent bonds, and to the fact that this high affinity is preserved as the ligand molecule is derivatized. Moreover, biotin association occurs to each monomeric unit within the holoprotein and results in the binding of two ligand molecules at each of two opposing interfaces of SA, enabling the implementation of complex cross-linking schemes for dedicated purposes (3, 4). Core SA has been crystallized and its structure has recently been solved (5, 6).

Despite the fact that biotechnological techniques using SA gain their sensitivity mainly from heterogeneous reaction schemes, the amount of direct information about the interaction of the protein at fluid interfaces has been limited due to the lack of sensitive surface analytical techniques applicable to such systems. This situation is now changing as a strong interest in liquid interfaces has been revived (7, 8). Fluorescence microscopy revealed that two-dimensional (2D) SA crystallization occurs underneath a surface monolayer of a biotin-functionalized lipid (9, 10). Electron microscopy of protein layers after transfer onto electron microscope grids disclosed structural information and showed unambiguously the formation of thin crystalline domains (11). We have employed the neutron reflectivity technique for the investigation of lipid monolayers (12) and of lipid/protein layer systems, using a dedicated liquid surface neutron reflectometer.

Address correspondence to Dr. M. Lösche.
Dr. Vaknin's current address is Iowa State University, Physics Department, Ames, Iowa 50011.

EXPERIMENTAL

Samples were prepared on a Wilhelmy film balance (12) in 0.5 M NaCl (p.a. grade) solution, pH = 7, using ultrapure water that was either Millipore-filtered (Bedford, MA) (H_2O) or five times distilled (D_2O) as described earlier (12). For a stock solution, streptavidin was diluted in D_2O at a concentration of 0.5 mg/ml from which 1 ml was added to the electrolytic subphase (400 ml) contained within the film balance. The isotopic purity of the D_2O was 98 ± 1%. A biotinylated lipid, compound 7 of reference 10 (see insert in Fig. 4), was spread from $CHCl_3$ to give a low surface coverage in the range of 1 molecule per 150 to 1,250 Å^2 in different experiments. The neutron reflection experiments were performed at ambient temperature. Identical results were obtained if the lipid was spread on a subphase-containing protein and if protein stock solution was injected into the subphase underneath a prespread target lipid monolayer. In control experiments, samples were prepared from fluorescently-(~1 FITC per SA) labeled protein (13) on a film balance that has a fluorescence microscope incorporated (14), and were visualized after polarized excitation with the help of a highly sensitive video equipment and standard image analysis techniques.

The fixed-wavelength ($\lambda = 4.6$ Å) reflectometer, located at the guide hall of the DR-3 reactor of Risø National Laboratory, enables measurement of the neutron reflectivity, R, of a horizontal surface in

0006-3495/91/12/1545/08 $2.00

the momentum transfer range, $Q_z = 0 - 0.3$ Å^{-1}. R is measured by tilting the incident beam with respect to the sample surface and monitoring the intensities of the incident and specularly reflected beam (12). The background is determined separately in an off-specular geometry for each Q_z value, and subtracted. Reflectivity values down to the range of 10^{-6} are thus accessible. The data collection takes ~12 h for the measurement of a whole reflectivity curve.

RESULTS

Protein binding to the interface

As indicated by fluorescence microscopy, FITC-labeled streptavidin remained intact if dissolved in a pure water subphase, and bound to the biotinylated interface. This was suggested from the observation of the fluorescence that was specifically emitted from the image plane as the microscope was focused on the interface. The micrograph, Fig. 1, shows the formation of H-shaped domains of FITC-SA underneath a preformed biotinylated lipid monolayer on 0.5 M NaCl in H_2O at ambient temperature. The excitation light was polarized along the long side of the frame and FITC was excited preferentially in those domains whose long axes were parallel to this polarization direction. Rotation of the polarizer leads to an optical contrast reversal, analogous to the polarized fluorescence observations reported earlier (9–11). The

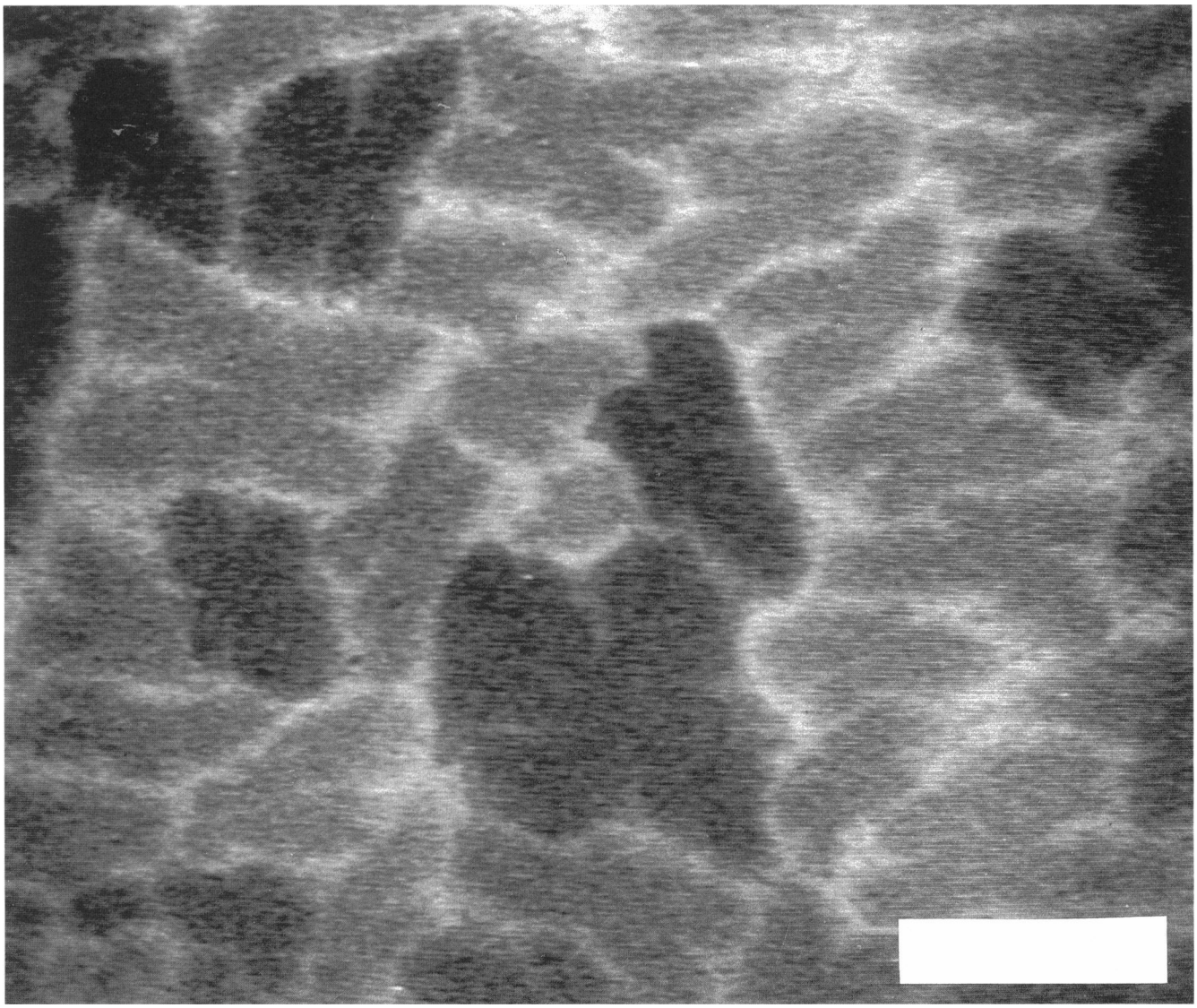

FIGURE 1 Fluorescence micrograph of phase separated domains of FITC-labeled streptavidin in 0.5 M NaCl/H_2O bound to a biotinylated lipid monolayer. The excitation light is linearly polarized parallel to the long axis of the frame. The bar corresponds to 50 μm.

formation of ordered domains that incorporate the chromophore with a preferred orientation was only observed at high ionic strength, in our case at 0.5 M NaCl. Immediately after the injection of the protein into the subphase, nucleation was observed and the whole surface was covered with domains within an hour.

We found significant differences between the H_2O and D_2O subphases under otherwise identical conditions. The nucleation in heavy water occurred even more efficiently than in light water, giving rise to smaller average domain sizes (i.e., higher nucleation densities) and to a higher surface coverage with protein domains. This dependence of the nucleation efficiency on the (heavy or light) water solvent shows the importance of hydrogen bonding in the formation of protein domains. Hydrogen bonds are apparently stronger in D_2O, an observation, which is consistent with earlier results on the interaction of polar lipid head groups with an aqueous subphase (12).

The neutron reflectivities from SA solutions in 0.5 M NaCl underneath monolayers of the biotin-functionalized lipid (200 $Å^2$/molecule) at $T = 18°C$ are shown in Fig. 2, *a* and *b* (D_2O subphase) and *b* (H_2O subphase). Included as solid lines are the expected reflectivities calculated from a model of the interface constructed as described below and refined by a simultaneous fit to both experimental data sets (12). Broken lines indicate the reflectivities of the pure (D_2O or H_2O) salt solutions. Due to the low surface density of the protonated lipid, the reflectivities of an aqueous surface and a lipid covered interface were experimentally indistinguishable. Fig. 2 *c* displays the scattering length density (SD) profiles normal to the interface that were used to generate the model reflectivities. In the D_2O experiment, two distinct profiles led to identical reflection intensities as discussed later.

Fig. 3 *a* shows the reduction of the reflectivity of the D_2O interface at $Q_z = 0.04$ $Å^{-1}$ upon protein binding. The detection arm of the instrument was horizontally rotated out of the specular reflection position to scan an angle, $2\Theta_H$, from $-3°$ to $3°$. Triangles show reflected neutron counts before protein injection underneath the prespread lipid monolayer; squares correspond to data taken ~1 h after protein injection. Count time per data point was 30 s. Best fits to Gaussian line shapes are included as guides for the eye. Protein binding to the interface led to a pronounced increase of the reflectivity at $Q_z = 0.03$ $Å^{-1}$ if H_2O was used as a subphase solvent (see Fig. 3 *b*).

Data interpretation

The changes in reflectivities of the water surfaces at low Q_z upon protein injection underneath the lipid monolayers, Fig. 3, demonstrates how the adsorption of protein to the surface can be monitored in situ. In addition, the pronounced structure in the reflectivity curves, Fig. 2, indicates the presence of a layered structure with a thickness, $d_p \sim 40$ Å, at the interface, as will be discussed below.

The neutron reflectivity of a stratified interface is to a good approximation (15, 16) proportional to the Fourier transform of the gradient of the scattering length density, ρ, projected onto the surface normal, *z* (17):

$$R(Q_z) = R_F(Q_z)\left|\frac{1}{\rho_{bulk}}\int \frac{d\rho(z)}{dz} * e^{iQ_z z}dz\right|^2.$$

R_F is the Fresnel reflectivity of a perfectly flat surface with a SD, ρ_{bulk}. Thus, the reflectivity provides direct information on the structure along one dimension, across the interface. Surface roughening was accounted for by a Gaussian smearing (rms roughness σ) of the SD function ρ.

For modeling the data we have introduced two slabs, or boxes, of constant scattering length densities which are intrinsically computed from the molecular content of a unit volume (which we chose to accommodate one SA tetramer) using standard values of the scattering lengths and taking into consideration the specific geometric constraints (12). One box, close to the water subphase, accommodates the protein, protein-bound water (D_2O or H_2O), the bound biotin moieties, and the hydrophilic lipid spacer and head groups. The second box, close to the gas phase, incorporates the hydrophobic lipid parts. This slab, however, has a negligible effect on the reflectivity due to the low surface concentration of the lipid and the small scattering length of the protonated chains, so that the effective model is essentially reduced to one box. This box is characterized by the effective thickness, d_p, of the protein layer and by the unit area, A_0. In the unit volume, n_w, water molecules are associated with one protein molecule, as well as $n_b = A_0/A_b$ biotin moieties of which a maximum of $n = 2$ are protein bound. A_b is the area per lipid molecule known from the amount of lipid spread at the interface. We optimized model parameters by computing the reflectivities for both, heavy and light water, subphases from the same geometric model in a composition-space refinement procedure. As we have shown (12), this formalism can easily be extended to refine models from neutron and x-ray reflectivity data concurrently. An analogous method has been used for the interpretation of x-ray and neutron diffraction data (18). Confidence limits on the resulting parameter values were determined as described in reference 12.

In this investigation we took the amino acid composi-

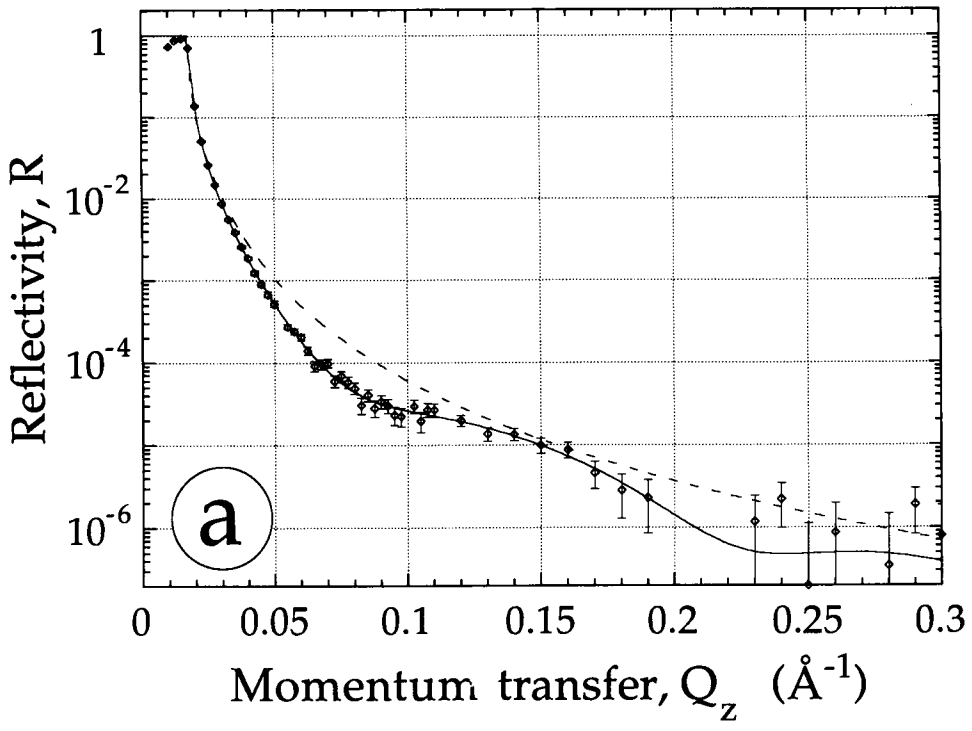

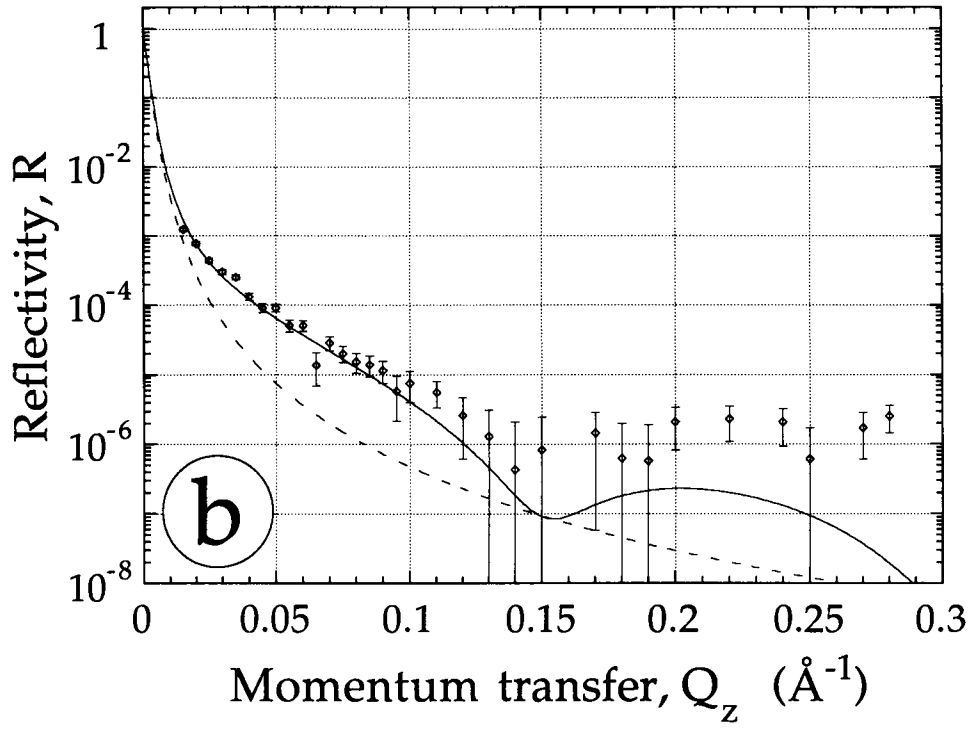

tion of the SA tetramer (2) and coupled it to the dry volume of the protein, which we estimated from its three-dimensional crystal unit cell size (6) to be, V_{SA}^{dry} = 111,500 Å^3. Using contrast variation, a joint refinement of the D_2O and H_2O data sets then enabled the determination of the amount of water associated with the protein. The difference in nucleation efficiency observed in our fluorescence microscopic observations was ac-

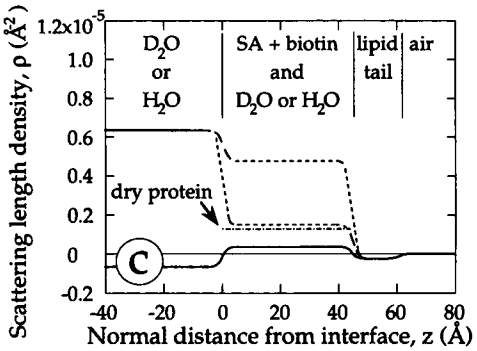

FIGURE 2 Neutron reflectivities, R, from the surface of a 0.5 M NaCl solution in D_2O (*a*) or H_2O (*b*) underneath a biotinylated surface layer versus momentum transfer, Q_z. Diamonds denote data taken with 10^{-8} M streptavidin in the solution. Solid lines correspond to the expected reflectivities calculated from the model; broken lines show the calculated reflectivities of the NaCl/water surfaces. (*c*) Neutron scattering length density profiles from which the reflectivities shown in *a* and *b* as solid lines were computed. In the D_2O case, two distinct SD profiles are depicted that lead to identical reflection intensities due to the phase problem. Out of these two, the one that is closer to the SD of the dry protein was connected with the shown H_2O SD profile in the joint refinement procedure. This correlation yielded a physically meaningful result.

counted for by introducing distinct surface coverage values, $P(D_2O)$ and $P(H_2O)$.[1]

In our attempt to evaluate the data, we found that the interface was best described in terms of one homogeneous protein monolayer directly located underneath the lipid, see Fig. 4. In particular, we have not resolved a water layer between the protein and the lipid at the surface, which indicates that the protein was tightly bound to ligand molecules protruding into the aqueous subphase. At the same time our model placed the protein at a well defined and strongly confined position with respect to the interface, and was in contrast to a diffuse layer expected if the driving force for adsorption is electrostatic interaction.

QUANTIFICATION OF RESULTS AND DISCUSSION

Independent of any model describing the stratified interface, the structure of the reflectivity curves in Fig. 2 demonstrates the formation of a layer of ~44 Å thickness, which has to be interpreted as a monolayer of adsorbed protein. When we modeled the experimental data sets independently, we found two scattering length density profiles corresponding to the situation of protein

[1]In practical terms, the parameters P and A_0 are coupled because water interpenetration between solid protein domains or between protein molecules within domains can only be distinguished if the coherence length of the probing beam has a value intermediate between the sizes of the protein domains and the protein molecules. In fact, however, the coherence is strongly anisotropic within the sample area (~100,000 Å in the direction of the beam projected on the surface and ~100 Å in the perpendicular direction). In the high contrast, full coverage situation (D_2O subphase), this is irrelevant, but in the low contrast, incomplete coverage situation (H_2O) this leads to an ambiguity. We decided to model the data using an assumption that A_0 is identical in both situations. This simplification may lead to an underestimation of the result for $P(H_2O)$ but has negligible influence on the other results which are strongly dominated by D_2O data set.

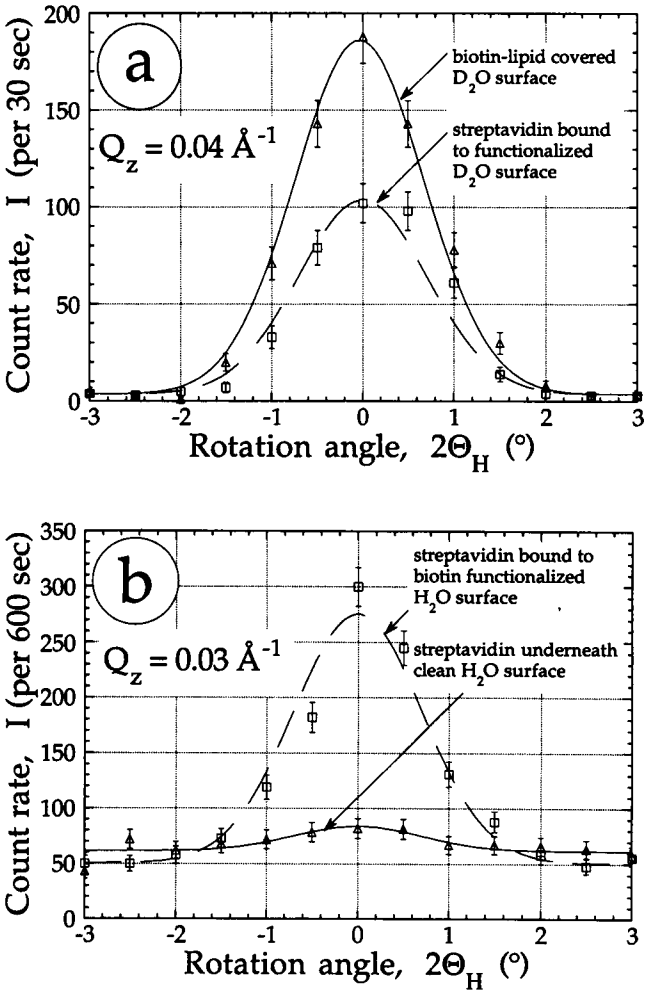

FIGURE 3 Reflected neutron counts from 0.5 M NaCl/water surfaces at constant Q_z versus horizontal rotation angle, $2\Theta_H$, out of the specular reflection position. (*a*) Squares and triangles show experimental data after and before protein injection underneath a biotinylated monolayer on D_2O; (*b*) squares and triangles show experimental data after and before spreading of a biotinylated monolayer on a streptavidin solution in H_2O. Lines are guides for the eye.

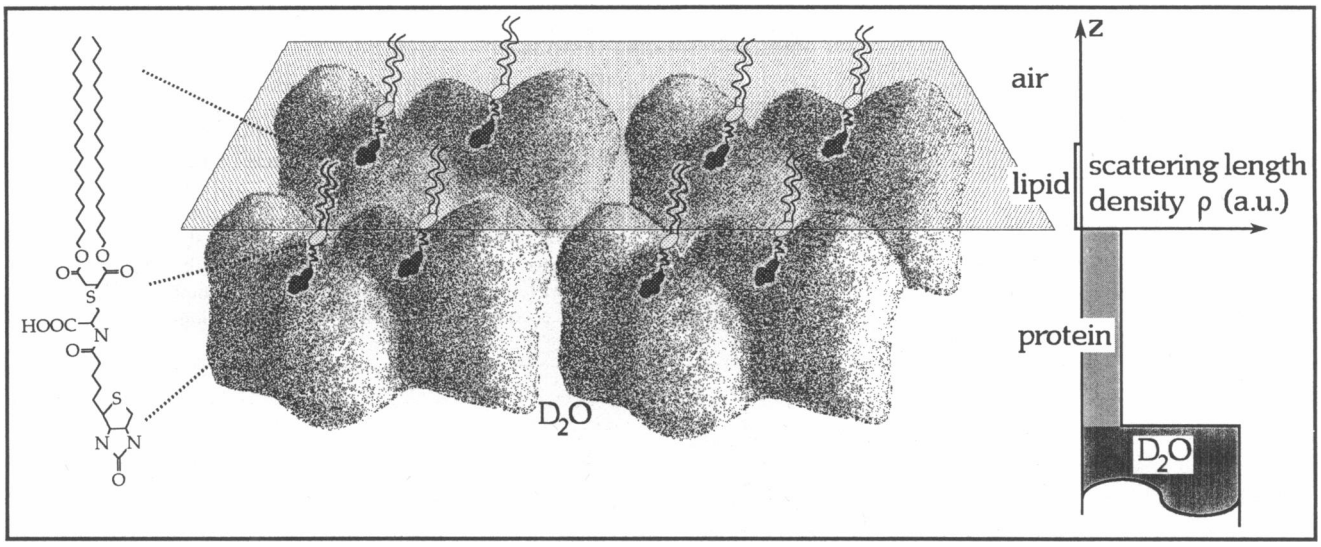

FIGURE 4 Schematic presentation of a streptavidin monolayer bound to biotinylated lipid (molecular structure displayed on the left) at the interface, according to the results listed in Table 1. Included on the right side is the corresponding scattering length density distribution across the interface (surface roughness omitted for clarity).

bound to the functionalized D_2O surface that fit the experimental data equally well as they produced identical model reflectivities. This is due to the lack of information on the phases of the reflected beams, and both situations are depicted in Fig. 2 *c*. However, both SD profiles lead to different conclusions regarding the in-plane packing of the protein monolayer. In the first model (*lower dashed line*), only a small amount of water interpenetrates the protein that is densely packed, whereas in the other case (*upper dashed line*), water occupies as much as 80% of the volume within the protein monolayer. Modeling the H_2O data set, Fig. 2 *b*, by itself, does not resolve this ambiguity. This is due to the fact that the low contrast between adjacent layers in the H_2O case (see Fig. 2 *c*) resulted in large uncertainties in the derived parameter values. However, the result from the joint refinement procedure described above led to the rejection of the model structure with the high water content as this corresponded to an unphysical situation, requiring $P(H_2O) \gg 1$. We will henceforth discuss the densely packed protein model as the most probable result.

Table 1 summarizes the structural quantities derived from the data and the constants used in the calculation. The upper part gives those parameters which have been treated as independent in the least-squares fit procedure. The value of the interface roughness, $\sigma = 2.6 \pm 2$ Å, is comparable to typical values observed with lipid covered surfaces (12). The protein layer thickness, $d_p = 43.7 \pm 2$ Å, and average area per protein molecule in the film, $A_0 = 2860 \pm 200$ Å, can be related to the geometry of the protein as obtained from the crystal structure (5, 6). Projected lengths of the tetramer on its molecular axis have been given as $P*Q*R = 54*58*48$ Å^3, respectively (6), and from the projections of the C^α backbone onto the PQ plane we estimate the limiting area for

TABLE 1 Structural parameters derived from the data of Fig. 2

Protein layer thickness	d_p	43.7 ± 2 Å*
Area of the unit cell	A_o	2860 ± 200 Å^2
Surface roughness	σ	2.6 ± 2 Å
Surface coverage values	$P(H_2O)$	0.4 ± 0.1
	$P(D_2O)$	1.0 ± 0.1
Number of water molecules	n_w	260 ± 100
Number of ligand molecules	n_b	14
Dry volume of protein‡	V_{SA}^{dry}	111,500 Å^3
Volume of water molecule	V_w	30 Å^3
Volume of biotin/spacer group§	V_b	400 Å^3
Surface area per biotin molecule‖	A_b	200 Å^2

Upper section, independent parameters determined from the best fit to the data; center section, dependent quantities; ¶lower section, constants used in the model.

*Confidence limits determined according to the procedure detailed in (12).

‡Estimated from the data in (6).

§Estimated from a comparison to the volume of a phospholipid head group (12); the model is very insensitive to this "parameter" as it is dominated by the larger protein volume.

‖Determined from the known amount of lipid spread at the interface.

¶$n_w = (A_o * d_p - V_{SA}^{dry} - n_b * V_b)/V_w$; $n_b = A_o/A_b$.

lateral close packing to be, $A_0^{min} \sim 2{,}350$ Å^2. The results obtained by electron microscopy of 2D crystals (11) places one protein molecule in an area of $A_0 = 3{,}570$ Å^2. For electron microscopy, films were prepared by protein incubation of a mixed monolayer at high biotin surface density, and stained with uranyl acetate after transfer (11). The resulting electron density map, Fig. 3 *c* in reference 11, shows close SA–SA contacts at rather small areas of the protein surface with large intervening regions that were presumably filled with interstitial water before uranyl staining. This electron density map supports a speculation that more compact 2D unit cells can easily be constructed by translation of the protein unit along its long axis toward its next nearest neighbor without violating geometric constraints. The result on A_0 that we obtained hints at the development of a different mutual arrangement of the SA molecules with our film preparation protocol. We have observed that still different preparation procedures may again lead to significantly different protein densities (unpublished results).

The value of the SA layer thickness, $d_p \sim 44$ Å, suggests that the bound protein assumes a slightly more oblate shape than in the crystal structure. Our results indicate an extreme geometric homogeneity of the bound protein layer and support the suggestion in reference 11 of the formation of a monomolecular protein layer. At the same time the small number of water molecules, $n_w \sim 260$, associated with each SA unit indicates intensive lateral contacts between the protein tetramers that may lead to the formation of 2D crystals. The amount of water found is probably near the lower limit of what is physically reasonable, as it would only support building up slightly more than one single monolayer of water molecules around the protein's surface in the film to separate it from its nearest neighbor. For comparison, a five times larger amount of water per protein by weight is estimated to be included in 3D crystals of sperm whale myoglobin (F. Parak, personal communication).

Using extremely low lipid surface concentrations in some experiments we found that as few as $n_b \sim 2.5$ biotin moieties per SA are sufficient to induce the growth of a protein monolayer. This shows that binding occurs quantitatively and reflects the exceptionally high affinity in this protein/receptor system.

CONCLUSIONS

We have demonstrated that the binding of a protein to a functionalized lipid monolayer can be monitored and characterized on a molecular length scale by analyzing the surface reflectivity for neutrons. Our data show specific binding between protein in an extremely dilute solution and receptor molecules at an interface at a comparably low density. The bound protein forms a monomolecular layer that is located directly at the interface. The dimensions of the protein molecules in the bound state have been assessed and their water content has been estimated. The technique enables systematic investigations of the formation of ligand/receptor complexes at model interfaces with the aim of controlling the binding characteristics via the optimization of the functionalized surface. It is promising to extend these measurements to similar x-ray investigations. From the joint refinement procedures that we have established (12), more detailed information, e.g., about the water distribution, can be expected. Similarly, kinetic measurements seem feasible, as in the low Q_z regime one can use large reflectivity differences between surfaces with or without protein bound to it. Finally, it is tempting to extend such experiments to sample preparations that implement complex cross-linking schemes thus exploiting the full versatility of the biotin/streptavidin system.

We are indebted to H. Ringsdorf for providing us with the biotinylated lipid and to K. Kjaer, H. Möhwald, and B. Buras for helpful discussions.

Financial support from the NOVO and Carlsberg foundations, the Danish Research Council, and the German Bundesministerium für Forschung und Technologie under contract No. 05 453 FA I9 is gratefully acknowledged.

Received for publication 17 April 1991 and in final form 30 July 1991.

REFERENCES

1. Chaiet, L., and F. J. Wolf. 1964. The properties of streptavidin, a biotin-binding protein produced by streptomycetes. *Arch. Biochem. Biophys.* 106:1–5.
2. Green, N. M. 1975. Avidin. *In* Advances in Protein Chemistry. M. L. Anson and J. T. Edsell, editors. Academic Press, New York. 85–133.
3. Bayer, E. A., and M. Wilchek. 1980. The use of the avidin-biotin complex as a tool in molecular biology. *Meth. Biochem. Anal.* 26:1–45.
4. Wilchek, M. and E. A. Bayer. 1988. The avidin-biotin complex in bioanalytical applications. *Anal. Biochem.* 171:1–32.
5. Weber, P. C., D. H. Ohlendorf, J. J. Wendolowski, and F. R. Salemme. 1989. Structural origins of high-affinity biotin binding to streptavidin. *Science (Wash. DC).* 243:85–88.
6. Hendrickson, W. A., A. Pähler, J. L. Smith, Y. Satow, E. A. Merritt, and R. P. Phizackerley. 1989. Crystal structure of core streptavidin determined from multiwavelength anomalous diffraction of synchrotron radiation. *Proc. Natl. Acad. Sci. USA.* 86:2190–2194.
7. Swalen, J. D., D. L. Allara, J. D. Andrade, E. A. Chandross, S.

Garoff, J. Israelachvili, T. J. McCarthy, R. Murray, R. F. Pease, J. F. Rabolt, K. J. Wynne, and H. Yu. 1987. Molecular monolayers and films. *Langmuir.* 3:932–950.

8. Möhwald, H. 1990. Phospholipid and phospholipid-protein monolayers at the air/water interface. *Annu. Rev. Phys. Chem.* 41:441–476.
9. Ahlers, M., R. Blankenburg, D. W. Grainger, P. H. Meller, H. Ringsdorf, and C. Salesse. 1989. Specific recognition and formation of two-dimensional streptavidin domains in monolayers: applications to molecular devices. *Thin Solid Films.* 180:93–99.
10. Blankenburg, R., P. H. Meller, H. Ringsdorf, and C. Salesse. 1989. Interaction between biotin lipids and streptavidin monolayers: formation of oriented two-dimensional protein domains induced by surface recognition. *Biochemistry.* 28:8214–8221.
11. Darst, S. A., M. Ahlers, P. H. Meller, E. W. Kubalek, R. Blankenburg, H. O. Ribi, H. Ringsdorf, and R. D. Kornberg. 1991. Two-dimensional crystals of streptavidin on biotinylated lipid layers and their interactions with biotinylated macromolecules. *Biophys. J.* 59:387–396.
12. Vaknin, D., K. Kjaer, J. Als-Nielsen, and M. Lösche. 1991. Structural properties of phosphatidylcholine at the air/water interface. Neutron reflection study and reexamination of x-ray reflection experiments. *Biophys. J.* 59:1325–1332.
13. Nargessi, R. D., and D. S. Smith. 1986. Fluorometric assays for avidin and biotin. *Methods Enzymol.* 122:67–73.
14. Lösche, M., and H. Möhwald. 1984. Fluorescence microscope to observe dynamical processes in monomolecular layers at the air/water interface. *Rev. Sci. Instrum.* 55:1968–1972.
15. Als-Nielsen, J. 1986. Synchrotron x-ray studies of liquid-vapour interfaces. *Physika.* 140A:376–389.
16. Penfold, J., R. K. Thomas, E. A. Simister, E. M. Lee, and A. R. Rennie. The structure of mixed surfactant monolayers at the air-liquid interface, as studied by specular neutron reflection. *J. Phys. Condens. Matter.* 2:411–416.
17. Als-Nielsen, J., and K. Kjaer. 1989. X-ray reflectivity and diffraction studies of liquid surfaces and surfactant monolayers. *In* Phase Transitions in Soft Condensed Matter. T. Riste and D. Sherrington, editors. Plenum Press, New York. 113–138.
18. Wiener, M. C., and S. H. White. 1991. Fluid bilayer structure determination by the combined use of x-ray and neutron diffraction II. "Composition-space" refinement method. *Biophys. J.* 59:174–185.